(2) (a) NDEA Trainee. (b) Camille and Henry Dreyfus Foundation Teacher-Scholar Grant Awardee, 1972–1977, and Fellow of the Alfred P. Sloan Foundation, 1973–1975.

(3) B. B. Chastain, E. A. Rick, R. L. Pruett, and H. B. Gray, *J. Amer. Chem. Soc.*, **90**, 3994 (1968).

(4) K. J. Coskran, J. M. Jenkins, and J. G. Verkade, *J. Amer. Chem. Soc.*, **90**, 5437 (1968).

(5) J. K. Stalick and J. A. Ibers, *Inorg. Chem.*, **8**, 1084 (1969).

(6) J. K. Stalick and J. A. Ibers, *Inorg. Chem.*, **8**, 1090 (1969).

(7) B. B. Chastain, D. W. Meek, E. Billig, J. E. Hix, Jr., and H. B. Gray, *Inorg. Chem.*, **7**, 2412 (1968).

(8) O. Dahl, *Acta Chem. Scand.*, **23**, 2342 (1969).

(9) J. W. Dawson, T. J. McLennan, W. Robinson, A. Merle, M. Dartiguenave, Y. Dartiguenave, and H. B. Gray, *J. Amer. Chem. Soc.*, **96**, 4428 (1974).

(10) J. A. Bertrand and D. L. Plymale, *Inorg. Chem.*, **5**, 879 (1966).

(11) C. G. Pierpont and R. Eisenberg, *Inorg. Chem.*, **11**, 828 (1972).

(12) E. F. Riedel and R. A. Jacobson, *Inorg. Chim. Acta*, **4**, 407 (1970).

(13) L. J. Vande Griend, J. M. Jenkins, and J. G. Verkade, in preparation.

(14) (a) R. A. Jacobson, "An Algorithm for Automatic Indexing and Bravais Lattice Selection, the Programs BLIND and ALICE," U.S. Atomic Energy Commission Report IS-3469, Iowa State University and Institute for Atomic Research, Ames, Iowa, 1974; (b) D. E. Williams, "LCR-2, a Fortran Lattice Constant Refinement Program", U.S. Atomic Energy Commission Report IS-1052, Iowa State University and Institute for Atomic Research, Ames, Iowa, 1964. The Nelson–Riley extrapolation function was used in the refinement.

(15) C. R. Hubbard, C. O. Quicksall, and R. A. Jacobson, "The Fast Fourier Algorithm and the Programs ALFF, ALFDP, ALFFPROJ, ALFFT, and FRIEDEL," U.S. Atomic Energy Commission Report IS-2625, Iowa State University and Institute for Atomic Research, Ames, Iowa, 1971.

(16) W. R. Busing, K. O. Martin, and H. A. Levy, "OR FLS, a Fortran Crystallographic Least-Squares Program," U.S. Atomic Energy Commission Report ORNL-TM-305, Oak Ridge National Laboratory, Oak Ridge, Tenn., 1962.

(17) H. P. Hanson, F. Herman, J. D. Lea, and S. Skillman, *Acta Crystallogr.*, **17**, 1040 (1964).

(18) "International Tables for X-Ray Crystallography," Vol. III, 2nd ed, Kynoch Press, Birmingham, England, 1962, pp 214–216.

(19) Supplementary material.

(20) C. A. Johnson, "OR TEP-II: A Fortran Thermal-Ellipsoid Plot Program for Crystal Structure Illustrations," U.S. Atomic Energy Commission Report ORNL-3794 (2nd Revision with Supplemental Instructions), Oak Ridge National Laboratory, Oak Ridge, Tenn., 1970. All drawings depict 30% probability ellipsoids.

(21) W. R. Busing, K. O. Martin, and H. A. Levy, "OR FFE, a Fortran Crystallographic Function and Error Program," U.S. Atomic Energy Commission Report ORNL-TM-306, Oak Ridge National Laboratory, Oak Ridge, Tenn., 1964.

(22) D. W. Meek and J. A. Ibers, *Inorg. Chem.*, **8**, 1915 (1969).

(23) K. N. Raymond, P. W. R. Corfield, and J. A. Ibers, *Inorg. Chem.*, **7**, 1362 (1968).

(24) L. Pauling, "Nature of the Chemical Bond," 3rd ed, Cornell University Press, Ithaca, N.Y., 1960, Chapter 7.

(25) R. J. Gillespie, *J. Chem. Soc.*, 4679 (1963).

(26) K. N. Raymond, D. W. Meek, and J. A. Ibers, *Inorg. Chem.*, **7**, 1111 (1968).

(27) J. H. Meiners, C. J. Rix, J. C. Clardy, and J. G. Verkade, *Inorg. Chem.*, preceding paper.

(28) D. L. Stevenson and F. D. Dahl, *J. Amer. Chem. Soc.*, **89**, 3424 (1967).

(29) Reference 24, p 260.

(30) E. L. Muetterties, W. Mahler, and R. Schmutzler, *Inorg. Chem.*, **2**, 613 (1963); E. L. Muetterties, W. Mahler, S. J. Packer, and R. Schmutzler, *ibid.*, **3**, 1298 (1964).

(31) J. E. Huheey, "Inorganic Chemistry: Principles of Structure and Reactivity," Harper and Row, New York, N.Y., 1972, Chapter 4.

(32) J. H. Meiners, J. C. Clardy, and J. G. Verkade, *Inorg. Chem.*, in press.

(33) M. J. Nolte and G. Gafner, *Acta Crystallogr., Sect. B*, **30**, 738 (1974).

(34) R. A. Marsh, J. Howard, and P. Woodward, *J. Chem. Soc., Dalton Trans.*, 778 (1973).

(35) A. D. U. Hardy and G. A. Sim, *J. Chem. Soc., Dalton Trans.*, 1900 (1972).

(36) R. M. Kirchner and J. A. Ibers, *Inorg. Chem.*, **13**, 1667 (1974).

(37) M. J. Nolte, G. Gafner, and L. M. Haines, *J. Chem. Soc. D*, 1406 (1969).

(38) F. H. Allen, G. Chang, K. K. Cheung, T. F. Lai, L. M. Lee, and A. Pidcock, *J. Chem. Soc. D*, 1297 (1970).

Contribution from the Chemistry Department,
University of Hawaii, Honolulu, Hawaii 96822

Crystal Structures of Acetylene Sorption Complexes of Partially Manganese(II)-Exchanged and Partially Cobalt(II)-Exchanged Forms of Zeolite A

PAUL E. RILEY and KARL SEFF*

Received April 29, 1974 AIC402797

The crystal structures of the acetylene sorption complexes of partially Mn(II)-exchanged and partially Co(II)-exchanged forms of the synthetic molecular sieve sodium zeolite 4A have been determined from three-dimensional X-ray diffraction data gathered by counter methods. Both structures were solved and refined in the cubic space group $Pm3m$; at 20 (1)° the cell constants are 12.205 (7) Å for the Mn(II) form, stoichiometry $Mn_{4.5}Na_3Al_{12}Si_{12}O_{48}\cdot 4.5C_2H_2$, and 12.171 (6) Å for the Co(II) form, stoichiometry $Co_4Na_4Al_{12}Si_{12}O_{48}\cdot 4C_2H_2$, per unit cell. Prior to the sorption of acetylene, activation of each zeolite was achieved in 48 hr at 1×10^{-6} Torr and elevated temperatures (350° for the Mn(II) form; 400° for the Co(II) form). In each structure, each transition metal ion lies on a threefold axis in the large central cavity of the unit cell, close to three equivalent trigonally arranged zeolite framework oxygen atoms (Mn(II)–O = 2.177 (10) Å, Co(II)–O = 2.193 (7) Å) and symmetrically to both carbon atoms of a C_2H_2 molecule (Mn(II)–C = 2.63 (17) Å, Co(II)–C = 2.54 (7) Å). At these latter distances, the interactions are weak, probably resulting from electrostatic attractions between the bivalent cations and the polarizable π-electron density of the acetylene molecules. The Na^+ ions of each structure occupy similar threefold axial positions (at sites not containing transition metal ions) which are somewhat recessed into the small sodalite cages (to distribute positive charge more uniformly), where nearly planar coordination to framework oxygen atoms is attained. No interaction between Na^+ ions and C_2H_2 molecules is observed in either structure. Full-matrix least-squares refinement has converged to a conventional R index (on F) of 0.065 for the Mn(II) system using 205 reflections for which $I_0 > 3\sigma(I_0)$ and 0.062 for the Co(II) structure using 297 similarly selected reflections.

Introduction

Utilization of the selective sorptive and catalytic properties of aluminosilicates is widespread.[1] The petroleum industry, for example, relies heavily upon aluminosilicates for the catalytic cracking of large hydrocarbon molecules. In fundamental research, a great variety of chemical reactions (isomerizations, polymerizations, dehydrogenations, and oxidations, for example) are conducted over aluminosilicate surfaces.[2] Consequently, considerable effort has been expended in determining the nature of the aluminosilicate sorptive and catalytic sites in order to learn about the physical forces operative in aluminosilicate catalysis, to postulate reaction mechanisms, perhaps to observe reaction intermediates, and, ultimately, to devise highly specific catalytic systems. Structural characterization, to which the crystalline zeolites are amenable, can be most useful in pursuing these objectives.

The work of Pickert, *et al.*,[3] with Y-type zeolites[4,5] indicates that bivalent cation exchange does indeed augment zeolite catalysis. Their studies show that isomerization of *n*-hexane is enhanced in the order Na–Y < Sr–Y < Ca–Y < Mg–Y. It appears that this catalytic activity varies monotonically with the polarizing power of the cation or with metal ion acidity, a property which increases with decreasing ionic radius. Several bivalent cations of the first transition series are similar in size to Mg^{2+}—the most active ion of the above series—and therefore these ions might be expected to exhibit similar or, because of the availability of d orbitals, perhaps higher catalytic activity.

Accordingly, a variety of reactions have been studied over transition metal exchanged zeolites. For example, the dehydrogenation of alkanes,[6] the conversion of alcohols to aldehydes and ketones,[7] and the oxidation of *n*-hexane to carboxylic acids[8-11] have been conducted (usually with yields increased by the exchange) over A- and X-type zeolites containing Cr(II), Mn(II), Fe(II), Co(II), or Ni(II) ions. Furthermore, the decomposition of ammonia (to N_2 and H_2),[12] the preparation of CH_4 from CO and H_2,[13] and the production of CO_2 from CO and O_2[14] have been carried out over bivalent transition metal ion–zeolite systems.

Clearly, zeolites, especially those containing transition metal ions, are capable of catalyzing a wide assortment of chemical reactions; in this sense, they resemble complex metalloenzyme systems. However, they differ from enzymes in some very important respects. Whereas the catalytic activities of enzymes are confined to narrow ranges of temperature and pH, zeolite catalysts function effectively over broad ranges for both of these variables.[15] Furthermore, the conformational flexibility of an enzyme contrasts sharply to the rigid, nearly uncompromising framework of a zeolite. Yet, despite the conformational freedom of a metalloenzyme, the transition metal ions, which are usually vital to its catalytic activity, may be compelled to satisfy their coordination requirements in somewhat unfavorable ways. By comparison, the positions to which the exchangeable zeolitic cations are directed by an unyielding anionic zeolite framework may represent locations of similar coordination strain. Hence, the exchangeable cations of a zeolite may bond with sorbed molecules in unusual ways, perhaps not unlike the binding and activation of coordinated functional groups in large biological systems.

Interesting and characterizable transition metal complexes do form intrazeolitically. By means of reflectance spectroscopy, Klier and Rálek[16,17] have studied complexes of Co(II) and Ni(II) with H_2O, NH_3, N_2O, and cyclopropane in A-type zeolite systems. Also, Boudart,[18] employing Mössbauer spectroscopy, has examined Fe(II) complexes of several small molecules (N_2, O_2, CO, pyridine, CS_2, alcohols, etc.) in Y-type zeolites.

Using the methods of single-crystal X-ray diffraction, the structural features of two partially ion-exchanged zeolite A systems—a Co(II) form[19] and a Mn(II) form[20]—have been elucidated in this laboratory. In these two systems it has been observed that upon dehydration (activation) the transition metal ions adopt positions close to the anionic zeolite framework where they achieve trigonal near-planar coordination. Subsequent treatment of the Co(II) form with carbon monoxide yields four-coordinate Co(II) ions; that is, each Co(II) ion maintains its trigonal framework bonds and also binds one molecule of CO.[19]

Study of these systems introduces some unusual crystallographic difficulties. At present synthetic zeolite single crystals are small, less than 0.01 cm along an edge. In addition, the sorbed molecules are usually few, often crystallographically disordered, and normally composed of light atoms. Hence, the contribution made by sorbed molecules to the diffracted X-ray intensities is small. Furthermore, the attractive forces between the cations and the sorbed molecules are often weak; and the cavities where these molecules reside are so large that the intermolecular forces usually existent in crystalline solids are appreciably diminished. Consequently, the small contribution made to the Bragg reflections by sorbed molecules is further attenuated by the resultant large thermal motion of these molecules.

As part of a continuing study to ascertain more precisely the effects of sorption upon transition metal exchanged zeolite systems (*i.e.*, to determine shifts in cation and framework atomic positions, to observe cation–sorbate interactions, and, perhaps to detect resultant changes in sorbed molecule geometry), the crystal structures of two zeolite A–acetylene complexes are reported: one of Mn(II), $Mn_{4.5}Na_3Al_{12}Si_{12}O_{48}\cdot 4.5C_2H_2$ per unit cell, $Mn_{0.375}Na_{0.25}[AlSiO_4]$–A·$0.375C_2H_2$ in conventional nomenclature;[21] and the other of Co(II), $Co_4Na_4Al_{12}Si_{12}O_{48}\cdot 4C_2H_2$ per unit cell, or $Co_{0.33}[AlSiO_4]$–A·$0.33C_2H_2$. A brief account of the Mn(II) system has been published.[22]

Experimental Section

Sample Preparation. Single crystals of the synthetic molecular sieve sodium zeolite 4A, stoichiometry $Na_{12}Al_{12}Si_{12}O_{48}\cdot 27H_2O$, form as colorless cubes. Recently Charnell[23] has reported the synthesis of crystals of this material with edge lengths as great as 0.01 cm, an acceptable size for single-crystal work. Ion exchange with 0.1 *M* Co(II) or Mn(II) solutions was conducted as described before[19,20] with crystals of zeolite 4A. After equilibrium was attained, elemental analyses indicated the stoichiometries $Co_4Na_4Al_{12}Si_{12}O_{48}\cdot xH_2O$ and $Mn_{4.5}Na_3Al_{12}Si_{12}O_{48}\cdot yH_2O$ per unit cell, subsequently designated Co_4–A and $Mn_{4.5}$–A (exlusive of water molecules).

One of the largest single crystals from each ion-exchange experiment was selected for X-ray diffraction studies; these had approximate edge lengths of 0.007 and 0.008 cm for the hydrated $Mn_{4.5}$–A and Co_4–A sieves, respectively. Each crystal was placed in a finely drawn Pyrex capillary, attached to a vacuum system, and then cautiously dehydrated (activated) by gradually incrementing its temperature (*ca.* 25°/hr) at a constant pressure of 5×10^{-4} Torr. When the Mn(II) and Co(II) samples reached temperatures of 350 and 400°, respectively, the pressure was reduced again, to less than 1×10^{-6} Torr. These conditions were maintained for 48 hr for each crystal.

After the crystals returned to ambient temperature (23°), each was treated with zeolitically dried acetylene (Matheson Gas Products), at pressures of 708 and 710 Torr for Co_4–A and $Mn_{4.5}$–A, respectively. Under these conditions, each crystal was removed in its capillary from the vacuum system by torch.

Microscopic examination indicated no apparent damage to either crystal, although dehydration and/or acetylene sorption induced dramatic color changes in both. In an earlier study,[19] it was determined that upon dehydration the Co_4–A crystal changed from pink-tan to deep blue, a color it has retained here, after treatment with acetylene. In contrast, both hydrated and dehydrated forms of $Mn_{4.5}$–A are pink-tan,[20] but sorption of acetylene has yielded a yellow-orange crystal.

X-Ray Data Collection. Previous crystallographic studies in this laboratory[5a] have indicated that the space group *Pm*3*m* (cubic system; no reflections systematically absent) is suitable, although it does not distinguish between the ordered Si and Al atoms and is therefore only approximately correct. Gramlich and Meier[24] have reported that for the hydrated unexchanged form of sodium zeolite 4A, the cubic space group $Fm\bar{3}c$ is appropriate. However, the few very weak superlattice reflections noted in this work for the Co(II) complex (indicative of an *F*-centered unit cell with a doubled lattice constant) do not show the systematic absences of $Fm\bar{3}c$.

Preliminary crystallographic experiments and subsequent data collections were performed with an automated, four-circle Syntex $P\bar{1}$ diffractometer, equipped with a graphite monochromator and a pulse height analyzer. Molybdenum radiation was used for all experiments ($K\alpha_1$, λ 0.70926 Å; $K\alpha_2$, λ 0.71354 Å). Cubic unit cell constants at 20 (1)°, as determined by a least-squares refinement of 15 intense reflections for which $20° < 2\theta < 24°$ (for both structures), are 12.205 (7) Å for $Mn_{4.5}$–A·$4.5C_2H_2$ and 12.171 (6) Å for Co_4–A·$4C_2H_2$.

For each crystal, reflections were measured by the θ–2θ technique at a constant scan speed of 0.5° min^{-1}. A symmetric scan range, from 1° (in 2θ) below the calculated $K\alpha_1$ peak to 1° above the $K\alpha_2$ peak, was used for every reflection. Background was examined at each end of the scan range for a time equal to half the reflection scan time. The intensities of three reflections in different regions of reciprocal space were recorded after every 100 reflections as a check on crystal

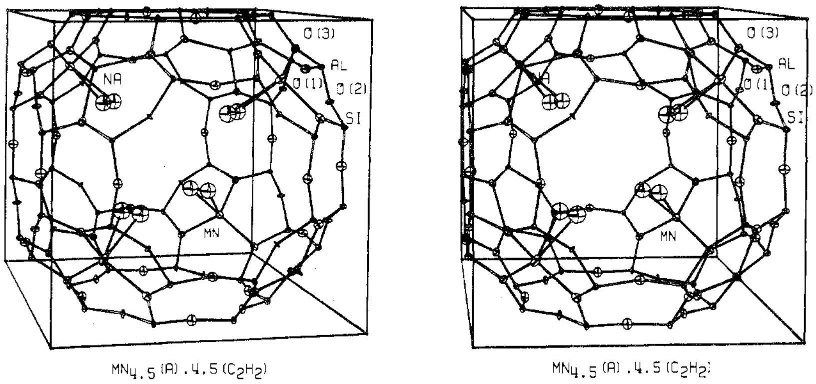

Figure 1. A stereoview of the $Mn_{4.5}$-A·4.5C_2H_2 unit cell. Heavy bonds indicate the approximate tetrahedral coordination about Mn(II). Ellipsoids of 20% probability are used. The disorder and uncertainties described in the text must be considered when viewing this idealized illustration.

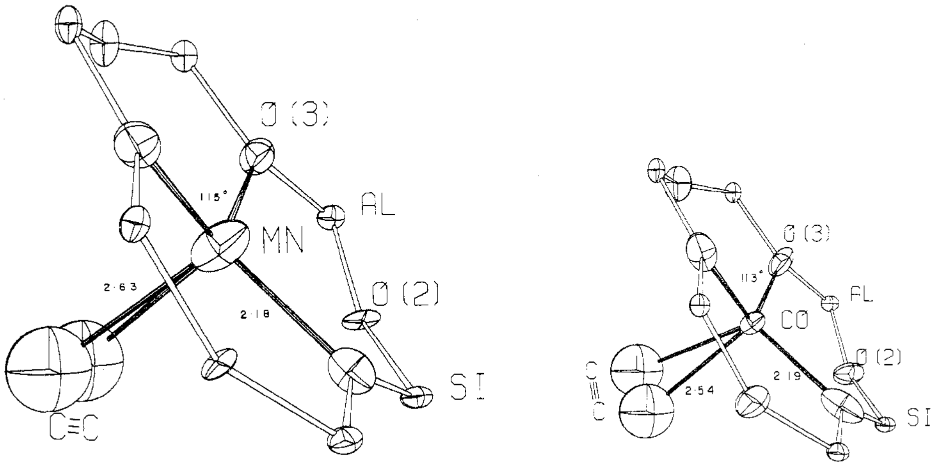

Figure 2. The coordination environments of the Mn(II) and Co(II) ions in each structure. Ellipsoids of 50% probability are used. The disorder and uncertainties described in the text must be considered when viewing these idealized illustrations.

and instrument stability. In each data set, a linear decline in intensity was observed, amounting in total to 5% of the initial values.

All reciprocal lattice points for which $2\theta < 70°$ were examined for each crystal. Although few reflections were significantly greater than background for high 2θ values, this limit was selected to maximize the size of these relatively small data sets.

Standard deviations were assigned in accordance with the expression

$$\sigma(I) = [\{CT + (0.25)(t_c/t_b)^2(B_1 + B_2)\}\omega^2 + (pI)^2]^{1/2}$$

where CT is the total integrated count obtained in a scan time t_c, B_1 and B_2 are the background counts each measured in time t_b, ω is the scan rate, and $I = [CT - 0.5(t_c/t_b)(B_1 + B_2)]\omega$. The value of p was taken as 0.02.[25] The usual corrections for Lorentz and polarization effects were applied, as well as small corrections for the decay mentioned above.[26] No absorption corrections were required: the linear absorption coefficients are 12.5 and 14.0 cm^{-1} for the Mn(II) and Co(II) systems, respectively; and in the same order, the transmission factors varied from 0.927 to 0.918 and 0.905 to 0.892. Only those reflections for which $I_0 > 3.0\sigma(I_0)$ were used[27] in structural analysis. For the Mn(II) system, 208 reflections of the 870 examined met this criterion, while for the larger Co(II)-containing crystal 302 of 862 reflections were regarded as observed. As the refinement of the Mn(II) structure approached convergence, three faint reflections (2,7,16, 2,8,16, and 5,6,12) appeared to be erroneously measured. These were discarded, yielding final data sets of 205 and 302 reflections.

It has been reported (see Discussion) that Co(II)-exchanged zeolite Y promotes the conversison of acetylene to benzene at or near room temperature.[28] From difference Fourier syntheses with our Co(II)-containing system, we observed electron density at a threefold axis position about 1 Å from the acetylenic carbon atoms. This minor peak was subsequently found to behave satisfactorily in least-squares refinement (although an isotropic thermal parameter of 20 Å^2 was required for an occupancy of 50%). To determine whether the sorbed acetylene molecules of this complex were undergoing a polymerization reaction during initial data collection, a second data set was acquired with the crystal 40 days later. Collection and reduction of the data were performed as described above, and a total of 297 reflections were judged to be significant (*i.e.* $I_0 > 3.0\sigma(I_0)$).

Refinement of both Co_4-A·4C_2H_2 data sets yielded equivalent structures; no reaction between acetylene molecules was detected from the second study. However, the second data set refined better than the first one: the standard deviations in bond lengths decreased slightly, and the conventional and weighted R indices (defined in the following section) decreased from 0.063 and 0.062 for the initial data set (supplementary Table II) to 0.062 and 0.057 for the second data set (supplementary Table III). Therefore, the discussion of the crystal structure of Co_4-A·4C_2H_2 is based upon the results obtained with the second data set.

Determination of the Structure of $Mn_{4.5}$-A·4.5C_2H_2. Full-matrix least-squares refinement was commenced using the framework atomic parameters ((Si,Al), O(1), O(2), and O(3)) and the Mn(II) parameters determined from the study of the fully hydrated species.[20] See Figures 1 and 2 (left) for the indentities of the atoms. (Because of the indistinguishability of SiO_4 and AlO_4 tetrahedra, only the average species, (Si,Al), is considered in our work.) Convergence was attained in three cycles with values for the discrepancy indices R_1 and R_2 of 0.13 and 0.14, respectively.

$$R_1 = \Sigma|F_o - |F_c||/\Sigma F_o$$

$$R_2 = (\Sigma w(F_o - |F_c|)^2/\Sigma w F_o{}^2)^{1/2}$$

The quantity minimized in the least-squares treatment was $(\sum w(F_o - |F_c|)^2)$[29] and the weights (w) were the reciprocal squares of $\sigma(F_o)$, the standard deviation of each observation. Atomic scattering factors for O^- and $(Si,Al)^{1.75+}$ for the zeolite framework and Na^+ and Mn(I) (or Co(II) in the subsequent structure) for the exchangeable cations were used.[30] The function describing $(Si,Al)^{1.75+}$ is the mean of the Si^0, Si^{4+}, Al^0, and Al^{3+} functions. The scattering factors for Mn^+, Co^{2+}, and $(Si,Al)^{1.75+}$ were modified to account for the real parts ($\Delta f'$) of the anomalous dispersion correction.[31]

Table I. Positional, Thermal, and Occupancy Parameters for $Mn_{4.5}$–A·4.5C_2H_2[a]

	Wyckoff position	x	y	z	β_{11} or B_{iso}	β_{22}	β_{33}	β_{12}	β_{13}	β_{23}	Occupancy factor
(Si,Al)	24 (k)	0	1814 (3)	3676 (2)	25 (2)	17 (2)	11 (2)	0	0	5 (3)	1[b]
O(1)	12 (h)	0	2008 (12)	5000	63 (13)	35 (12)	45 (10)	0	0	0	1
O(2)	12 (i)	0	2962 (6)	2962 (6)	46 (10)	12 (4)	12 (4)	0	0	21 (10)	1
O(3)	24 (m)	1129 (5)	1129 (5)	3255 (8)	35 (4)	35 (4)	40 (7)	18 (9)	−13 (8)	−13 (8)	1
Mn	8 (g)	2074 (5)	2074 (5)	2074 (5)	55 (4)	55 (4)	55 (4)	38 (8)	38 (8)	38 (8)	$^{4.5}/_8$
Na	8 (g)	1579 (16)	1579 (16)	1579 (16)	24 (7)	24 (7)	24 (7)	36 (19)	36 (19)	36 (19)	$^3/_8$
C	48 (n)	3031 (94)	3334 (162)	3534 (139)	9 (4)[c]						$^3/_{16}$

[a] Positional and anisotropic thermal parameters are given ×10⁴. Numbers in parentheses are the estimated standard deviations in the units of the least significant digit given for the corresponding parameter. See Figure 1 for the identities of the atoms. The anisotropic temperature factor is $\exp[-(\beta_{11}h^2 + \beta_{22}k^2 + \beta_{33}l^2 + \beta_{12}hk + \beta_{13}hl + \beta_{23}kl)]$. [b] Occupancy for (Si) = ½; occupancy for (Al) = ½. [c] Isotropic thermal parameter in units of Å².

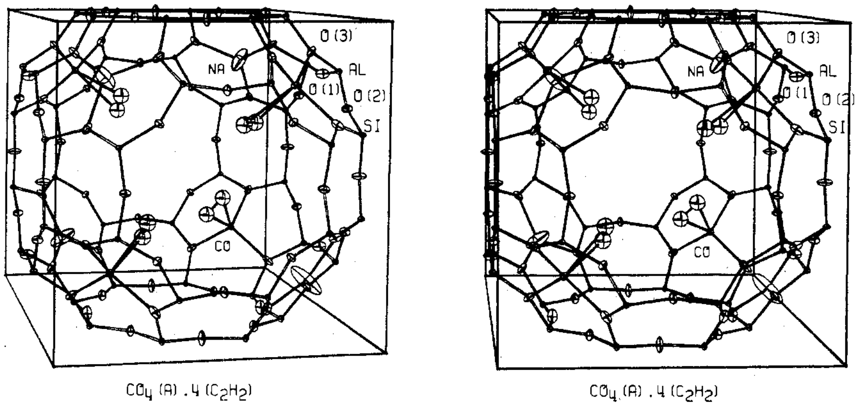

Figure 3. A stereoview of the Co_4–A·4C_2H_2 unit cell. Heavy bonds indicate the approximate tetrahedral coordination about Co(II). Ellipsoids of 20% probability are used. The caution in the preceding figure captions applies.

A difference Fourier synthesis at this juncture indicated probable positions for the Na^+ ions (just inside the small cages or sodalite units and distributed over an eightfold equipoint) and for the carbon atoms of the C_2H_2 molecules (in the large cage). Inclusion of 3 Na^+ ions and 4.5 C_2H_2 molecules (using a C (valence) scattering function[30]) in the next sequence of isotropic refinement yielded convergence with $R_1 = 0.084$ and $R_2 = 0.094$. Decreasing the carbon occupancy by a factor of 2 yielded unreasonably small thermal parameters. Further refinement employing anisotropic thermal parameters for all species except acetylene molecules converged with $R_1 = 0.065$ and $R_2 = 0.067$. The goodness of fit, $(\sum w(F_o - |F_c|)^2/(m - s))^{1/2}$, is 1.03 where m (205) is the number of observations and s (31) is the number of variables in least-squares refinement. In the final cycle of least-squares refinement, all shifts in atomic parameters were less than 0.4% of their corresponding standard deviations. A final difference Fourier map revealed two peaks: one at the origin (3.4 (1) e Å^{-3}) and one (2.0 (1) e Å^{-3}) on the threefold axis at the Mn(II) ion. The origin peak, which has been encountered in other zeolite crystal studies, has been discussed previously[20b] and is too distant from the rest of the structure to be bonded even weakly to it. For comparison, on the initial difference map the height of the Na^+ ions was 5.6 (1) e Å^{-3} for an occupancy of 37.5%.

Final positional, thermal, and occupancy parameters are presented in Table I; bond lengths and bond angles are given in Table II. A listing of $10F_o$ and $10F_c$ is available.[32]

Determination of the Structure of Co_4–A·4C_2H_2. Solution and least-squares refinement of this structure was conducted generally as discussed in the preceding section. See Figure 3 for a stereoview of the unit cell. Isotropic refinement using framework and cation positional and thermal parameters determined in an earlier study[19] of the dehydrated Co_4–A sieve converged quickly with R_1 and R_2 = 0.10. Full anisotropic refinement reduced R_1 to 0.076 and R_2 to 0.073. The acetylene molecules were then readily located in the large cavity from a difference Fourier function, and inclusion of four molelcules of C_2H_2 with isotropic thermal parameters in least-squares refinement converged with $R_1 = 0.062$, $R_2 = 0.057$, and a goodness of fit of 1.19 for 31 parameters (s) and 297 observations (m). In the last cycle of least-squares refinement, no parameter changed by more than 1.7% of its estimated standard deviation. Two peaks were observed on a subsequent difference Fourier synthesis: a peak of 2.31 (1) e Å^{-3} at the origin, which was dismissed as before, and a peak of height 1.0 (1) e Å^{-3} along the unit cell threefold axis close to the acetylene molecules, which was not well behaved in least-squares refinement.

Table II. Interatomic Distances (Å) and Angles (deg)[a]

	$Mn_{4.5}$–A·4.5C_2H_2	Co_4–A·4C_2H_2
	Distances	
(Si,Al)–O(1)	1.633 (4)	1.633 (2)
(Si,Al)–O(2)	1.650 (5)	1.647 (3)
(Si,Al)–O(3)	1.692 (4)	1.687 (3)
M–O(3)[b]	2.177 (10)	2.193 (7)
M–O(2)[b]	2.959 (6)	2.973 (4)
Na–O(3)	2.188 (13)	2.120 (7)
Na–O(2)	3.067 (13)	2.995 (11)
M–C[b]	2.63 (17)	2.54 (7)
C–C	0.9 (3)	1.16 (12)
	Angles	
O(1)–(Si,Al)–O(2)	113.6 (5)	112.2 (3)
O(1)–(Si,Al)–O(3)	111.8 (3)	111.8 (4)
O(2)–(Si,Al)–O(3)	105.0 (5)	105.9 (4)
O(3)–(Si,Al)–O(3)	109.0 (6)	108.9 (4)
(Si,Al)–O(1)–(Si,Al)	163.4 (4)	162.8 (3)
(Si,Al)–O(2)–(Si,Al)	153.8 (8)	151.6 (6)
(Si,Al)–O(3)–(Si,Al)	135.5 (6)	136.0 (4)
O(3)–M–O(3)[b]	114.9 (7)	113.3 (4)
O(3)–M–O(2)[b]	59.9 (4)	59.8 (2)
O(3)–Na–O(3)	114.0 (5)	119.6 (26)
O(3)–Na–O(2)	57.7 (3)	59.8 (9)
O(3)–M–C[b]	95.5 (26)	94.8 (15)
O(3)–M–C′[b,c]	102.0 (30)	102.4 (16)
O(3)–M–C[b]	112.0 (37)	117.9 (16)
C–C′–M[b,c]	80.5 (4)	76.7 (8)
C–M–C′[b,c]	19 (8)	27 (3)

[a] Numbers in parentheses are the estimated standard deviations in the units of the least significant digit given for the corresponding parameter. [b] M represents Mn(II) or Co(II). [c] The coordinates of a primed atom are related to those given in Table I or III by a threefold axis operation.

Table III. Positional, Thermal, and Occupancy Parameters for Co_4–A·$4C_2H_2$[a]

	Wyckoff position	x	y	z	β_{11} or B_{iso}	β_{22}	β_{33}	β_{12}	β_{13}	β_{23}	Occupancy factor
(Si,Al)	24 (k)	0	1818 (2)	3673 (1)	25 (1)	21 (1)	14 (1)	0	0	5 (2)	1[b]
O(1)	12 (h)	0	2022 (9)	5000	97 (10)	59 (8)	19 (5)	0	0	0	1
O(2)	12 (i)	0	2980 (5)	2980 (5)	63 (7)	26 (3)	26 (3)	0	0	17 (8)	1
O(3)	24 (m)	1129 (4)	1129 (4)	3256 (5)	56 (3)	56 (3)	41 (4)	60 (7)	−34 (6)	−34 (6)	1
Co	8 (g)	2111 (3)	2111 (3)	2111 (3)	32 (2)	32 (2)	32 (2)	14 (3)	14 (3)	14 (3)	$^1/_2$
Na	8 (g)	1778 (31)	1778 (31)	1778 (31)	255 (38)	255 (38)	255 (38)	453 (82)	453 (82)	453 (82)	$^1/_2$
C	48 (n)	2903 (41)	3357 (59)	3572 (58)	6 (2)[c]						$^1/_6$

[a] Positional and anisotropic thermal parameters are given ×10^4. Numbers in parentheses are the estimated standard deviations in the units of the least significant digit given for the corresponding parameter. See Figure 3 for the identities of the atoms. The anisotropic temperature factor is $\exp[-(\beta_{11}h^2 + \beta_{22}k^2 + \beta_{33}l^2 + \beta_{12}hk + \beta_{13}hl + \beta_{23}kl)]$. [b] Occupancy for (Si) = $^1/_2$; occupancy for (Al) = $^1/_2$. [c] Isotropic thermal parameter in units of Å^2.

Bond lengths and bond angles are in Table II; final positional, thermal, and occupancy parameters are given in Table III. Observed and calculated structure factors for both Co_4–A·$4C_2H_2$ data sets (see Experimental Section) are available.[32]

Table IV. Deviations of Atoms (Å) from the (111) Plane at O(3)[a]

	$Mn_{4.5}$–A (dehydrated)[b]	$Mn_{4.5}$–A·$4.5C_2H_2$
Mn	−0.11 (4)	0.50 (2)
Na	0.46 (4)	−0.55 (3)
O(2)	0.29 (4)	0.29 (3)
C		3.1 (2)

	Co_4–A (dehydrated)[c]	Co_4–A·4CO[c]	Co_4–A·$4C_2H_2$
Co	0.34 (5)	0.53 (4)	0.58 (2)
Na	−0.56 (4)	−0.58 (4)	−0.13 (6)
O(2)	0.29 (4)	0.33 (3)	0.31 (3)
C		2.8 (3)	3.0 (1)

[a] Numbers in parentheses are the estimated standard deviations in the units of the least significant digit given for the corresponding parameter. A negative deviation indicates that the atom lies on the same side of the plane as the origin. [b] See ref 20. [c] See ref 19.

Discussion of the Structures

$Mn_{4.5}$–A·$4.5C_2H_2$. Dehydration (activation) of a zeolite obviously alters its structure and hence its properties dramatically. Noteworthy changes in bond lengths and bond angles are observed[5a,19,20] as cation–framework and cation–cation electrostatic interactions intensify upon zeolite activation. The sorption of most molecules (but not water or ammonia, for example, which "fill" the zeolite with polar hydrogen-bonded networks that so moderate the electrostatic fields that the zeolite returns to a relaxed conformation) causes small zeolite changes, which for the most part are localized at the active sites, namely, near the exchangeable cations. Hence, a measure of the strength of sorbate binding is indicated not only by metal–sorbate separation but also by the more subtle changes in metal–framework interactions which must accompany metal–sorbate bond formation.

A comparison of the structure of $Mn_{4.5}$–A·$4.5C_2H_2$ with that of the "empty-sieve," $Mn_{4.5}$–A,[20] reveals two significant changes. In $Mn_{4.5}$–A, the Mn(II) ions are recessed slightly into the sodalite cages along the unit cell threefold axes, where they achieve trigonal near-planar coordination with three equivalent framework oxygen atoms, O(3)'s (see Figures 1 and 2 (left)). To interact with acetylene the Mn(II) ions pass through their planes of O(3) atoms into the large central cavity, a shift in position of 0.60 Å (see Table IV). In response to the movement of the highly charged Mn(II) ions, the Na^+ ions move a substantially greater distance (0.99 Å) along the threefold axes in the opposite direction (*i.e.*, from sites in the central cavity into the sodalite units). Although each Mn(II) (as well as each Na^+) remains tightly bound to its three nearest oxygen atoms, the binding to acetylene does weaken the interaction with the framework: in the fully dehydrated form, Mn–O(3) = 2.11 (1) Å;[20] in the acetylene complex, Mn–O(3) = 2.18 (1) Å. In contrast, the Na^+–O(3) bond lengths are essentially unchanged: Na^+–O(3) distances are 2.16 (5) and 2.19 (1) Å in the dehydrated and acetylated forms, respectively. In addition to the elongation of Mn–O(3) bonds, the effect of acetylene coordination is reflected in a change of O(3)–Mn–O(3) angle, from the nearly planar value of 119.6 (1)° to 114.9 (7)°—halfway in angle (and approximately 70% in required linear shift) to tetrahedral. No changes in the angles formed at Na^+ ions are observed. With the exception of an increase of 3° in the (Si,Al)–O(1)–(Si,Al) angle, no significant change in framework structure has resulted from acetylene sorption.

The exchangeable cation to O(3) distances presented here have not taken into account the probable but unobservable (due to disorder) differences in position of two sets of O(3) oxygen atoms: one set coordinated to the Mn(II) ions, and the other to the Na^+ ions; only the average ring of framework atoms is determined. Thus, we believe that the Mn–O(3) distance is slightly less than reported here, and Na–O(3), somewhat greater.

Of real interest is the interaction between the Mn(II) ions and the acetylene molecules (see Figure 2 (left)). A three-dimensional Fourier map, generated with phases determined by framework atoms, Mn(II) ions, and Na^+ ions only, indicated a broad somewhat toroidal volume of electron density centered on and orthogonal to the unit cell threefold axes, about 2.5 Å from Mn(II). The distance to the Na^+ ions would be 4.4 Å, too long to be an interaction; accordingly all of the acetylene molecules represented by this "torus" are associated with Mn(II) ions.

An attempt, partially successful, was made to resolve individual acetylene molcules further. The initial difference electron density function, sampled in Figure 4, argues strongly for a high degree of disorder, perhaps approaching entirely free rotation of C_2H_2 about an axis normal to its molecular axis and coincident with the threefold axis of the unit cell. Indeed, from esr measurements Naccache, *et al.*,[33] have observed that nitric oxide molecules bound to Cu(II) ions in Cu(II)-exchanged Y-type zeolite systems rotate about the Cu(II)–N axis. Furthermore, Cramer[34] has inferred from solution nmr studies that the ethylene molecules of π-$C_5H_5Rh(C_2H_4)_2$ probably rotate about the rhodium(I)–ethylene bond axes. In $Mn_{4.5}$–A·$4.5C_2H_2$, the acetylene molecules are held, as will be discussed below, less firmly than in any molecular complex reported; thus they are likely to be at least as mobile as the C_2H_4 molecules of the Rh(I) species.

The difference Fourier function also suggests that all nine acetylenic carbon atoms are crystallographically equivalent and that they statistically occupy an equipoint on diagonal mirror planes at $x = y = 0.304$ and $z = 0.336$, the two carbon atoms in the vicinity of each Mn(II) being distributed among the three equivalent positions depicted in Figure 4, with each

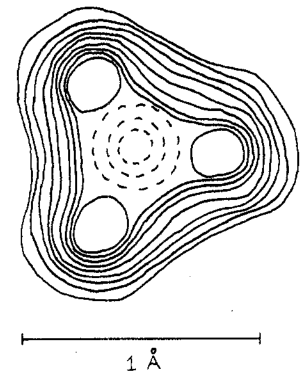

Figure 4. The electron density function for $Mn_{4.5}$-A·4.5C_2H_2 in the plane normal to the threefold axis at $x = 0.31$, through the maximum of this peak. Contours are drawn at intervals of 0.1 e $Å^{-3}$, and the electron density maximum corresponds to 1.6 e $Å^{-3}$. Dashed contours at the center represent decreasing electron density. The standard deviation of the electron density is calculated to be 0.12 e $Å^{-3}$.

corresponding acetylene molecular axis perpendicular to a diagonal mirror plane. The acetylene molecules are, then, in threefold disorder about each Mn(II). However, the requirement that each carbon atom lie on a mirror plane, as Figure 4 suggests, is inconsistent with the C_s symmetry, at most, of the molecular sorption site. Of course, a position near such a mirror plane might occur and apparently has. Least-squares refinement of the position (of higher symmetry) noted on the Fourier function, at x, x, z, converged successfully but yielded a very short C≡C bond, only 0.6 Å.

Least-squares refinement of a model with two types of carbon atoms occupying sites of m symmetry was carried out next. The nine carbon atoms were distributed equally between positions x, x, z ($x < z$) and x', z', z' ($x' < z'$); this corresponds to three equivalent molecular sites, each with nonequivalent C's and each approximately perpendicular to and intersecting the threefold axis. The least-squares treatment converged with R indices identical with those determined for the model described in the preceding paragraph but yielded thermal parameters which differed considerably for these two sites. For positions x, x, z and x', z', z' the thermal parameters are 3 (3) and 10 (4) $Å^2$, respectively, confirming as Figure 4 indicates, that x, x, z is better defined than x', z', z'. This model is therefore considered to be poor.

When the carbon atoms were moved slightly off the mirror planes as the molecular site symmetry of the first model suggests, to a general equipoint (x, y, z) and then refined by least squares, the nine carbon atoms could be assigned to positions within that equipoint to give a substantially improved C≡C distance, 0.9 (3) Å. In addition, the isotropic thermal parameter fell from 11 (4) $Å^2$ for the x, x, z model to 9 (4) $Å^2$, but the error indices rose from R_1 and $R_2 = 0.060$, to 0.065 and 0.067, respectively, and the diagonal anisotropic thermal parameter of Mn(II) increased by 5 esd's. Clearly, the disorder of the acetylene molecules is not easily described.

With all carbon atoms distributed about one general equipoint, each C_2H_2 molecule would again be composed of two equivalent carbon atoms. Since each position x, y, z is equivalent by the symmetry of this space group to five additional positions by the operation $3m$, six such peaks should have appeared in these regions on the previous difference Fourier function. However, as shown by Figure 4, only three peaks are observed, perhaps because y and z are close in value (see Table I).

In the better two of the above models, the acetylene molecular axis does not intersect a unit cell threefold axis; the center of a C≡C bond is about 0.3 Å from a threefold axis. However, if the two carbon atoms of each C_2H_2 molecule were to occupy two nonequivalent general positions x, y, z, and x', y', z') which differed in orientation by inversion at a point on the threefold axis, then the

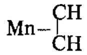
$$\mathrm{Mn}-\overset{\mathrm{CH}}{\underset{\mathrm{CH}}{\|}}$$

bond axis and the unit cell threefold axis would coincide. Least-squares refinement of such a model failed convincingly however; the carbon positions shifted greatly, the thermal parameters became unrealistic, and the R indices soared. Consequently, this model was rejected handily in favor of the noncoincident one.

The most satisfactory solution then, is that with all nine carbon atoms at one general position x, y, z. At these sites each C≡C bond is bisected by the diagonal mirror plane which relates one carbon atom of a C_2H_2 molecule to the other. As stated above, while the difference Fourier synthesis suggests that the carbon atoms are located on these diagonal mirror planes, least-squares refinement indicates that a more acceptable bond length can be obtained if the carbons are positioned off these planes.

The value determined for the carbon–carbon triple bond for this equivalent carbon atom description is 0.9 (3) Å, too short to be correct but understandable as an aberration resulting from thermal motion foreshortening and from unresolved disorder. In gaseous acetylene the C≡C distance is 1.201 (5) Å,[35] and in an acetylene complex of zeolite 4A,[36] the bonds are imprecisely determined (for the same reasons as discussed here) to be 1.03 (15) and 0.92 (10) Å.

Each carbon atom at x, y, z is 2.63 (17) Å from an Mn(II) ion, so that each C_2H_2 molecule approaches an Mn(II) ion symmetrically. (This distance is approximately independent of the model; it is a feature of the "torus".) No structural results suitable for quantitative comparison to this manganese complex could be located. However, for M(0)–C_2H_2 complexes, where M is a first-row transition metal, metal–carbon distances of 2.0 Å are generally observed.[37] We conclude that the binding in this complex is weak and probably results from the electrostatic interaction between the dipositive Mn(II) ions and the polarizable π-electron density of the C_2H_2 molecules. The high charge of the Mn(II) ions severely inhibits the synergic bonding[38] usually ascribed to symmetric metal–alkyne complexes, *i.e.*, donation of π-electron density of acetylene into an empty σ-acceptor orbital of the metal and "back-donation" of accumulated charge from metal d or dp hybrid orbitals into π-acceptor orbitals of acetylene.

Acetylene apparently functions solely as an electron donor, perhaps as it does in π-$C_5H_5Mn(CO)_2C_2(CF_3)_2$.[39] Infrared studies of this compound have shown that the acetylenic stretching frequency is only slightly affected by complexation, indicating that its triple-bond character is retained. In contrast, the C–C triple bond of most monoacetylene complexes of platinum[40] is so altered that it closely resembles a C–C double bond.

Perhaps what is observed in this zeolite complex is an approximate isolation of the σ portion of what would become a σ–π synergic bond, were the metal uncharged and therefore capable of back-donation so as to strengthen the interaction. Angell and Schaffer[41] have suggested from ir studies that this σ effect alone may account for the binding of carbon monoxide by Co(II) in X- and Y-type zeolites.

Although the uncertainty in the C–C bond is great, apparently no significant nonbonded approaches are made by acetylene to the zeolite framework. The closest such approach for C is 3.5 Å to an O(3) oxygen atom. The hydrogen atoms, although unlocated, should lie in the plane of the carbon positions. This plane is parallel to that of the nearest framework oxygens, the O(3)'s, 3.1 Å away (see Table IV), so the H···O distances cannot be less. Thus, the acetylenic hydrogens are far from framework oxygens, and no C–H···O hydrogen bonding occurs.[42]

Co_4–A·$4C_2H_2$. Dehydration induces migration of the Co(II) ions along the threefold axes from positions far from the framework in the hydrated form (the closest approach being 2.86 (3) Å to O(3) atoms) to positions in the large cavity on the threefold axes where nearly trigonal-planar coordination to O(3) atoms is achieved. In the dehydrated structure, the Co–O(3) bond is 2.08 (2) Å[19] and probably because of d-orbital asphericity the Co(II) ions lie somewhat further from their triangular coordination planes than do the spherical Mn(II) ions, the deviations from these planes being 0.34 (5) Å for Co(II) and 0.11 (4) Å for Mn(II) (see Table IV). Sorption of acetylene elicits a similar response for the Co(II) sieve as observed with the Mn(II) system; each Co(II) moves away from its plane of O(3) atoms into the central cage to bind one molecule of the gas (see Figures 2 (right) and 3). Bonding with the framework is maintained, and, as in the Mn(II) system, the bonds from transition metal ion to framework oxygen have lengthened, while the Na^+–framework distances are unchanged: Co–O(3) = 2.08 (2) Å and Na–O(3) = 2.12 (2) Å in Co_4–A; Co–O(3) = 2.193 (7) Å and Na–O(3) = 2.120 (7) Å in Co_4–A·$4C_2H_2$.

Sorption of carbon monoxide by Co_4–A yields a Co^{II}–CO complex which is apparently of intermediate nature. The Co–O(3) bond is 2.11 (2) Å,[19] perhaps slightly longer than in Co_4–A but shorter than in Co_4–A·$4C_2H_2$; correspondingly, the distance of a Co(II) ion from its O(3) plane is perhaps greater with C_2H_2 (0.58 (2) Å) than with CO (0.53 (4) Å). The accompanying changes in Na^+ positions, on the other hand, differ appreciably—0.43 Å with C_2H_2 but only 0.02 Å with CO (see Table IV).

The angles formed by the metal–framework bonds reflect these small changes in bond length; the angle O(3)–Co–O(3) is 117 (1)° in the dehydyrated sieve, 113.3 (4)° with sorbed acetylene, and 114 (1)° with sorbed carbon monoxide. In the same order the O(3)–Na–O(3) angles are 113 (1), 120 (3), and 113 (1)°. Changes in other framework and cation features common to the three forms of the Co(II) sieve are small and in nearly every instance insignificant as well. Bond lengths and bond angles for the Co_4–A·$4C_2H_2$ system are given in Table II. The reservations regarding exchangeable cation to O(3) distances, especially Na^+–O, stated in the discussion of $Mn_{4.5}$–A·$4.5C_2H_2$, apply to the Co(II) systems also.

A difference Fourier function, prepared from the contributions of all species except the four acetylene molecules, exhibited a broad ring of electron density normal to the threefold axes, just as had been noted before with $Mn_{4.5}$–A·$4.5C_2H_2$, although for this structure the positions of the carbon atoms are better resolved (see Figure 5). Nevertheless, the standard deviations of all bond lengths and bond angles formed with the acetylene molecules attest to the large uncertainties in carbon positions resulting from the combined effects of high thermal motion and probable high disorder.

The coordination geometry about Co(II) differs very little from that about Mn(II) as described above. One acetylene molecule is symmetrically bound to each Co(II) ion, and, as in the Mn(II) structure, the C≡C bond does not intersect the threefold axis; its center lies about 0.3 Å from that axis. The Co^{II}–C distance of 2.54 (7) Å appears shorter than the corresponding Mn^{II}–C distance (2.63 (17) Å), consistent with the difference in ionic radii, 0.72 Å for Co(II) and 0.80 Å for Mn(II). In a study of the acetylene sorption complex with the unexchanged form of sodium 4A,[36] the Na^+ to acetylene distance is 2.78 (10) Å. Again, this greater distance is probably a consequence of the larger radius of the Na^+ ion (0.95 Å). Furthermore, esr studies[43] indicate that the stronger electrostatic fields normally associated with smaller, more highly charged transition metal ions are somewhat diminished in the anionic zeolite environment, so that the strength of these sorption interactions may be correspondingly reduced.

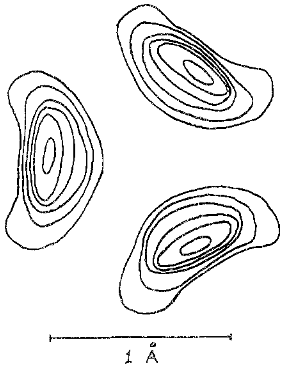

Figure 5. The electron density function for Co_4–A·$4C_2H_2$ in the plane normal to the threefold axis at $x = 0.32$, through the maximum of this peak. Contours are drawn at intervals of 0.1 e Å^{-3}, and the electron density maximum corresponds to 1.5 e Å^{-3}. The standard deviation of the electron density is calculated to be 0.11 e Å^{-3}.

The crystal structures of several cobalt–acetylene complexes indicate that acetylene can symmetrically bridge cobalt atoms. In $[(CO)_6Co_2C_2H]_3As$[44] the mean of six cobalt–acetylene Co–C distances is 1.96 Å, exactly as it is in $(CO)_6Co_2C_2(C_6H_5)_2$.[45] (Both structures exhibit significant C–C (acetylene) bond elongation, 1.32 Å for the first complex and 1.46 Å for the second. Such lengthening implies extensive delocalization of electron density over metal–acetylene π orbitals, as might be expected for the shorter metal–carbon distances observed in these complexes.)

Evidence that some zeolite catalytic processes are influenced by metal d electrons has been presented by Kruerke,[28] who studied the conversion of acetylene to benzene over several transition metal exchanged Y-type zeolites at undisclosed pressures. Trimerization was influenced by these cations, in the order Mn(II) ≪ Co(II) = Ni(II) ≫ Cu(II) = Zn(II). He pointed out that metal ions with two filled or two half-filled d orbitals are most active. Hence, back-bonding from the metal may indeed be of some importance in certain intrazeolitic reactions. No indication of this reaction was noted in the work herein reported.

Little difference in bond angles at the Co(II) and Mn(II) ions is noted (see Table III). Bonding between the Co(II) ions and the C_2H_2 molecules is probably due to the same mechanism discussed for the Mn(II) system, *i.e.*, electrostatic attraction of the polarizable π-electron density of the C_2H_2 molecules by the Co(II) cations. The determination of the acetylene triple bond for this Co(II) complex (1.16 (12) Å), though suffering from the disorder previously described, is more satisfactory than in the Mn(II) study, although its associated error is still large.

There is no indication of Na^+–C_2H_2 interaction in this structure. If a Na^+ ion, which is slightly recessed (by 0.13 (6) Å) into the sodalite cages, and a C_2H_2 molecule were to coexist in the same octant of the unit cell, then the Na^+–C distance would be 3.2 Å, too great to indicate a meaningful interaction.

The carbon atoms are no closer than 3.5 Å from the framework oxygen atoms, and any possible acetylenic hydrogen atom position would be greater than 3.0 Å (Table IV) from the nearest oxygen, O(3), as discussed in the preceding section. Accordingly, no bonded or hydrogen-bonded[42] interactions between acetylene and the zeolite framework are seen.

The possibility that the Co(II) and Na^+ ions have long-range order, tetrahedrally placed with respect to each large cavity or (equivalently) sodalite unit, so that $P\bar{4}3m$ would be a more suitable space group, was carefully considered[46] in Co_4Na_4–A·4C_2H_4 and was dismissed. Accordingly, since the structures are so similar, $P\bar{4}3m$ was not used in this work. The stoichiometry of Co_4Na_4–A is approximate; it is not an exchange limit; no physical evidence indicates an ordered structure has formed at room temperature.

Sorption measurements indicate that approximately seven molecules of acetylene are present in zeolites Na–A[47] and Ca–A[48] at 700 Torr and 298°K. Approximately six C_2H_2's were located in the crystal structure of the Na–A complex,[36] and the structures herein reported suggest that each of the six Ca^{2+} ions per unit cell could bind a C_2H_2 molecule in Ca–A. However, fewer molecules, none besides those associated with the transition metal ions, were located in either of the structures herein reported. Note, however, that C_2H_2 sorption has caused the divalent cations to shift into the large cavity and, to preserve electrostatic balance, the sodium ions to move in the opposite direction to positions at which coordination to C_2H_2 is unlikely. Accordingly, it appears that partial exchange of Na^+ with M(II) has decreased the capacity of the zeolite for C_2H_2 under these conditions.

Note Added in Proof. Esr results[49] suggest that the equipoint with the elongated Mn(II) thermal ellipsoid in dehydrated $Mn_{4.5}$–A[20] should have been resolved into two Mn(II) equipoints, one on each side of the six-rings and fractionally occupied so as to avoid very close ionic contacts. If that is correct, the structure model of dehydrated $Mn_{4.5}$–A[20] used here for comparison would be somewhat incorrect. The proper description of Mn(II) behavior upon C_2H_2 sorption would instead be that all Mn(II) ions have located at just one equipoint on the large cavity sides of the six-rings, instead of that they all have shifted their position from one equipoint of near-trigonal-planar symmetry at the centers of the elongated ellipsoids.[20] The crystallographic data for dehydrated $Mn_{4.5}$–A are by themselves unable to distinguish between the two possibilities, and so the less-detailed fewer-parameter solution was reported.[20]

Acknowledgment. This work was supported by the National Science Foundation (Grant No. GP-38639X). We are also indebted to Mr. Kevin B. Kunz for performing the ion-exchange experiments and to the University of Hawaii Computing Center.

Registry No. $Mn_{4.5}$-A·4.5C_2H_2, 54100-70-8; Co_4-A·4C_2H_2, 54100-69-5.

Supplementary Material Available. Listings of structure factor amplitudes will appear following these pages in the microfilm edition of this volume of the journal. Photocopies of the supplementary material from this paper only or microfiche (105 × 148 mm, 24× reduction, negatives) containing all of the supplementary material for the papers in this issue may be obtained from the Journals Department, American Chemical Society, 1155 16th St., N.W., Washington, D.C. 20036. Remit check or money order for $3.00 for photocopy or $2.00 for microfiche, referring to code number AIC402797.

References and Notes

(1) Detailed accounts of the properties and structures of molecular sieve zeolites are available: *Advan. Chem. Ser.*, **No. 101, 102** (1971); **No. 121** (1973).

(2) A well-referenced summary of aluminosilicate-catalyzed organic reactions is given by P. B. Venuto, pp 260–283 of **No. 102** of ref 1.

(3) P. E. Pickert, J. A. Rabo, E. Dempsey, and V. Schomaker, *Proc. Int. Congr. Catal. 3rd, 1964*, **1**, 714 (1965).

(4) Zeolite systems are discussed and illustrated by W. M. Meier and D. H. Olson, pp 155–170, **No. 101** of ref 1.

(5) A discussion of zeolite nomenclature is available: (a) R. Y. Yanagida, A. A. Amaro, and K. Seff, *J. Phys. Chem.*, **77**, 805 (1973); (b) L. Broussard and D. P. Shoemaker, *J. Amer. Chem. Soc.*, **82**, 1041 (1960).

(6) P. B. Venuto and P. S. Landis, *Advan. Catal.* **18**, 259 (1968).

(7) L. V. Pansevich-Kolyada and N. F. Ermolenko, *Russ. J. Phys. Chem.*, **40**, 1282 (1966).

(8) J. Rouchaud and J. Fripiat, *Bull. Soc. Chim. Fr.*, 78 (1969).

(9) J. Rouchaud, L. Sondegam, and J. J. Fripiat, *Bull. Soc. Chim. Belg.*, 505 (1968).

(10) J. Rouchard, P. Mulkay, and J. Fripiat, *Bull. Soc. Chim. Belg.*, 537 (1968).

(11) J. Rouchard, L. Sondegam, and J. J. Fripiat, *Bull. Soc. Chim. Fr.*, 4387 (1968).

(12) Reference 6, p 365.

(13) D. W. Breck, *J. Chem. Educ.*, **41**, 678 (1964).

(14) J. N. Miale and P. B. Weisz, U. S. Patent 3,136,713 (1964).

(15) Reference 1, **No. 102**, p 280.

(16) K. Klier and M. Ralek, *J. Phys. Chem. Solids*, **29**, 951 (1968).

(17) K. Klier, *J. Amer. Chem. Soc.*, **91**, 5392 (1969).

(18) W. N. Delgass, R. L. Garten, and M. Boudart, *J. Phys. Chem.*, **73**, 2970 (1969).

(19) P. E. Riley and K. Seff, *Inorg. Chem.*, **13**, 1355 (1974).

(20) (a) R. Y. Yanagida, T. B. Vance, Jr., and K. Seff, *J. Chem. Soc., Chem. Commun.*, 382 (1973); (b) R. Y. Yanagida, T. B. Vance, Jr., and K. Seff, *Inorg. Chem.*, **13**, 723 (1974).

(21) R. M. Barrer, paper presented at the Third International Conference on Molecular Sieves, Zurich, 1973.

(22) P. E. Riley and K. Seff, *J. Amer. Chem. Soc.*, **95**, 8180 (1973).

(23) J. F. Charnell, *J. Cryst. Growth*, **8**, 291 (1971).

(24) V. Gramlich and W. M. Meier, *Z. Kristallogr., Kristallgeometrie, Kristallphys., Kristallchem*, **133**, 134 (1971).

(25) S. W. Peterson and H. A. Levy, *Acta Crystallogr.*, **10**, 70 (1957).

(26) A. Christensen, LPCOR computer program, Syntex Analytical Instruments, 1970; T. Ottersen, LP-73 computer program, University of Hawaii, 1973.

(27) A. J. C. Wilson, *Acta Crystallogr., Sect. B*, **29**, 1488 (1973).

(28) J. A. Rabo and M. L. Poutsma, ref 1, **No. 102**, p 297.

(29) Principal programs used: full-matrix least squares, P. K. Gantzel, R. A. Sparks, and K. N. Trueblood, UCLALS4, American Crystallographic Association Program Library (old) No. 317 (modified); Fourier program, C. R. Hubbard, C. O. Quicksall, and R. A. Jacobson, Ames Laboratory Fast Fourier, Iowa State University, 1971; C. K. Johnson, ORTEP, Report ORNL-3794, Oak Ridge National Laboratory, Oak Ridge, Tenn., 1965.

(30) "International Tables for X-Ray Crystallography," Vol. III, Kynoch Press, Birmingham, England, 1962, p 212.

(31) C. H. Dauben and D. H. Templeton, *Acta Crystallogr.*, **8**, 841 (1955).

(32) Supplementary material.

(33) C. Naccache, M. Che, and Y. Ben Taarit, *Chem. Phys. Lett.*, **13**, 109 (1972).

(34) R. Cramer, *J. Amer. Chem. Soc.*, **86**, 217 (1964).

(35) L. E. Sutton, "Interatomic Distances and Configuration in Molecules and Ions," Supplement, The Chemical Society London, 1965, p S16s.

(36) A. A. Amaro and K. Seff, *J. Phys. Chem.*, **77**, 906 (1973).

(37) References contained in W. Hubel, "Organic Syntheses *via* Metal Carbonyls," Vol. 1, Interscience, New York, N.Y., 1968, p 273.

(38) A discussion of synergic bonding as related to metal–acetylene complexes is available: F. A. Cotton and G. Wilkinson, "Advanced Inorganic Chemistry," 3rd ed Interscience, New York, N.Y., 1972, p 749.

(39) J. L. Boston, S. O. Grim, and G. Wilkinson, *J. Chem. Soc.*, 3468 (1963).

(40) The structure of a Pt(II) complex presented in the following source is an example of symmetric metal–alkyne bonding: G. R. Davies, W. Hewertson, R. H. B. Mais, P. G. Owston, and C. G. Patel, *J. Chem. Soc. A*, 1873 (1970).

(41) C. L. Angell and P. C. Schaffer, *J. Phys. Chem.*, **70**, 1413 (1966).

(42) W. C. Hamilton and J. A. Ibers, "Hydrogen Bonding in Solids," W. A. Benjamin, New York, N.Y., 1968, p 16.

(43) Y. Huang, J. E. Benson, and M. Boudart, *Ind. Eng. Chem., Fundam.*, **8**, 346 (1969).

(44) P. H. Bird and A. R. Fraser, *J. Chem. Soc., Chem. Commun.*, 681 (1970).

(45) W. G. Sly, *J. Amer. Chem. Soc.*, **81**, 18 (1959).

(46) P. E. Riley, K. B. Kunz, and K. Seff, *J. Amer. Chem. Soc.*, **97**, 537 (1975).

(47) D. W. Breck, W. G. Eversole, R. M. Milton, T. B. Reed, and T. L. Thomas, *J. Amer. Chem. Soc.*, **78**, 5963 (1956).

(48) D. W. Breck, "Zeolite Molecular Sieves," Wiley, New York, N.Y., 1974, p 610.

(49) L. G. Dzhasiashvili, N. N. Tikhomirova, and G. V. Tsitsishvili, *Zh. Strukt. Khim.*, **8**, 453 (1967).